The EMBO Journal (2004) 23, 969–979 | © 2004 European Molecular Biology Organization | All Rights Reserved 0261-4189/04
www.embojournal.org

THE EMBO JOURNAL

Runx3 regulates mouse TGF-β-mediated dendritic cell function and its absence results in airway inflammation

Ofer Fainaru[1], Eilon Woolf[1], Joseph Lotem[1], Merav Yarmus[1], Ori Brenner[2], Dalia Goldenberg[1], Varda Negreanu[1], Yael Bernstein[1], Ditsa Levanon[1], Steffen Jung[3] and Yoram Groner[1,*]

[1]Department of Molecular Genetics, The Weizmann Institute of Science, Rehovot, Israel, [2]Department of Veterinary Resources, The Weizmann Institute of Science, Rehovot, Israel and [3]Department of Immunology, The Weizmann Institute of Science, Rehovot, Israel

Runx3 transcription factor regulates cell lineage decisions in thymopoiesis and neurogenesis. Here we report that Runx3 knockout (KO) mice develop spontaneous eosinophilic lung inflammation associated with airway remodeling and mucus hypersecretion. Runx3 is specifically expressed in mature dendritic cells (DC) and mediates their response to TGF-β. In the absence of Runx3, DC become insensitive to TGF-β-induced maturation inhibition, and TGF-β-dependent Langerhans cell development is impaired. Maturation of Runx3 KO DC is accelerated and accompanied by increased efficacy to stimulate T cells and aberrant expression of β2-integrins. Lung alveoli of Runx3 KO mice accumulate DC characteristic of allergic airway inflammation. Taken together, abnormalities in DC function and subset distribution may constitute the primary immune system defect, which leads to the eosinophilic lung inflammation in Runx3 KO mice. These data may help elucidate the molecular mechanisms underlying the pathogenesis of allergic airway inflammation in humans.
The EMBO Journal (2004) **23,** 969–979. doi:10.1038/sj.emboj.7600085; Published online 5 February 2004
Subject Categories: molecular biology of disease; immunology
Keywords: airway inflammation; knockout mice; lung eosinophilia; Runx3 transcription factor; TGF-β signaling

Introduction

The mammalian RUNX3 belongs to the runt domain family of transcription factors that are key regulators of lineage-specific gene expression in major developmental pathways. Expression of *RUNX* genes is controlled at the transcriptional level by two promoters and at the translational level by IRES and Cap-dependent translation control (Ghozi *et al*, 1996; Geoffroy *et al*, 1998; Pozner *et al*, 2000; Bangsow *et al*, 2001; Levanon *et al*, 2001b; Stewart *et al*, 2002). The RUNX proteins recognize the same DNA motif in target genes and activate or repress transcription through recruitment of other transcriptional modulators (Levanon *et al*, 1998; Ito, 1999). Despite this occurrence, each RUNX has well-defined biological functions reflected in a unique spatio/temporal expression pattern and by the fact that each of the corresponding knockout (KO) mice has a distinct phenotype (Karsenty, 2000; Levanon *et al*, 2001a, 2002; Speck, 2001; Inoue *et al*, 2002; Li *et al*, 2002).

Of the mammalian *RUNX* genes, *RUNX3* is the smallest, has the fewest number of exons (Bangsow *et al*, 2001) and emerged as the evolutionary founder of the mammalian *RUNX* gene family (Levanon *et al*, 2003). Expression of Runx3 was previously detected in various B- and myeloid cell lines (Levanon *et al*, 1994, 1996; Shi and Stavnezer, 1998; Le *et al*, 1999; Bangsow *et al*, 2001), but the *in vivo* function of Runx3 in these hematopoietic lineages has not been characterized. In the developing mouse embryo, Runx3 is expressed in hematopoietic organs, epidermal appendages, developing bones and sensory ganglia (Levanon *et al*, 2001a). Studies in KO mice revealed that Runx3 is a neurogenic specific transcription factor required for development and survival of the dorsal root ganglia TrkC neurons (Inoue *et al*, 2002; Levanon *et al*, 2002). Runx3 KO mice also display defects in thymopoiesis (Taniuchi *et al*, 2002; Woolf *et al*, 2003) and in the control of cell proliferation and apoptosis of gastric epithelium (Li *et al*, 2002).

DC are sparsely distributed, migratory bone-marrow-derived cells that are specialized in uptake, processing and presentation of antigens to T cells (Banchereau and Steinman, 1998; Steinman, 1999). The murine DC compartment is defined by surface expression of major histocompatibility complex class II (MHC II) and the β2-integrin CD11c, which is found on all DC, except Langerhans cells (LC). The latter are a specialized class of DC, which reside in the epidermis and whose development is uniquely dependent on the cytokine transforming growth factor β (TGF-β) (Borkowski *et al*, 1996).

At the immature state, DC monitor the antigenic environment for the presence of microorganisms. Detection of damage or pathogen-associated molecular patterns (PAMPs), such as lipopolysaccharides (LPS) and double-stranded RNA by tissue-resident DC, initiates DC maturation and migration to lymph nodes. Maturation is associated with upregulation of MHC II molecules and costimulatory molecules such as CD80 and CD86 (Banchereau and Steinman, 1998). Mature DC are unrivaled in their potential to stimulate naïve T cells.

The mucosal surfaces of the respiratory and intestinal tracts are constantly exposed to environmental antigens. In order to prevent overt inflammation, activation of antigen-presenting cells (APC) at these sites was proposed to be continuously attenuated by immunosuppressive cytokines such as TGF-β (Nathan, 2002). Supporting this notion,

*Corresponding author. Department of Molecular Genetics, The Weizmann Institute of Science, Rehovot 76100, Israel.
Tel.: +972 8 934 3972; Fax: +972 8 934 4108;
E-mail: yoram.groner@weizmann.ac.il

Received: 15 October 2003; accepted: 18 December 2003; Published online: 5 February 2004

absence of TGF-β was reported to result in lung inflammation (Nathan, 2002).

Numerous studies highlight the involvement of DC in the development of eosinophilic airway inflammation and asthma (Holt, 2000; Lambrecht *et al*, 2000; Umetsu *et al*, 2002). More recent data suggest a particularly critical role for a distinct subset of alveolar DC. These DC capture airborne antigens and maintain the capacity to activate specific T cells long after antigen exposure (Julia *et al*, 2002). In steady state, these cells comprise a minor fraction of alveolar cells, but they expand considerably in the lungs with ongoing Th2 immune responses (Julia *et al*, 2002).

Here we report that Runx3 is highly expressed in DC where it functions as a component of the TGF-β signaling cascade. When Runx3 is lost, epidermal LC are absent and KO DC display accelerated maturation, increased potency to stimulate T cells as well as aberrant expression of β2-integrins. Runx3 KO mice develop spontaneous eosinophilic lung inflammation, indicating an over-response to otherwise innocuous airborne antigens. This conclusion is supported by the increased abundance in the KO lungs of a unique subset of alveolar DC. Intriguingly, human RUNX3 resides in a region on chromosome 1p36.1 (Levanon *et al*, 1994; Bae *et al*, 1995) that contains susceptibility genes for asthma and hypersensitivity against environmental antigens (Haagerup *et al*, 2002). Thus, RUNX3 deficiency may constitute an asthma risk factor in humans.

Results

Runx3 KO mice develop spontaneous eosinophilic airway inflammation

Inbred Runx3-deficient mice are not viable and homozygous KO mice have therefore been maintained on outbred genetic background (Levanon *et al*, 2002). When screening our Runx3 KO mouse colony, we noticed that 52% (20/38) of 1- to 8-week-old naïve outbred KO mice (ICR, MF1 background) displayed a prominent eosinophil infiltration in their lungs, which was absent from the lungs of wild-type (WT) littermates. Infiltrating cells, which also contained mononuclear phagocytes and, less commonly, lymphocytes were most consistently encountered in the interstitium around blood vessels and airways (Figure 1A and B), typically involving 2–3 lung lobes. Vascular cuffs composed of an essentially purely eosinophilic population were present in many KO mice (Figure 1C and D), and in severe cases eosinophils and mononuclear cells expanded into the adjacent alveolar septae and filled the alveolar spaces. In some mice, perivascular and peribronchial inflammatory infiltration was accompanied by airway epithelial hyperplasia, mucus hypersecretion and excess collagen deposition (Figure 1E–H), indicating airway

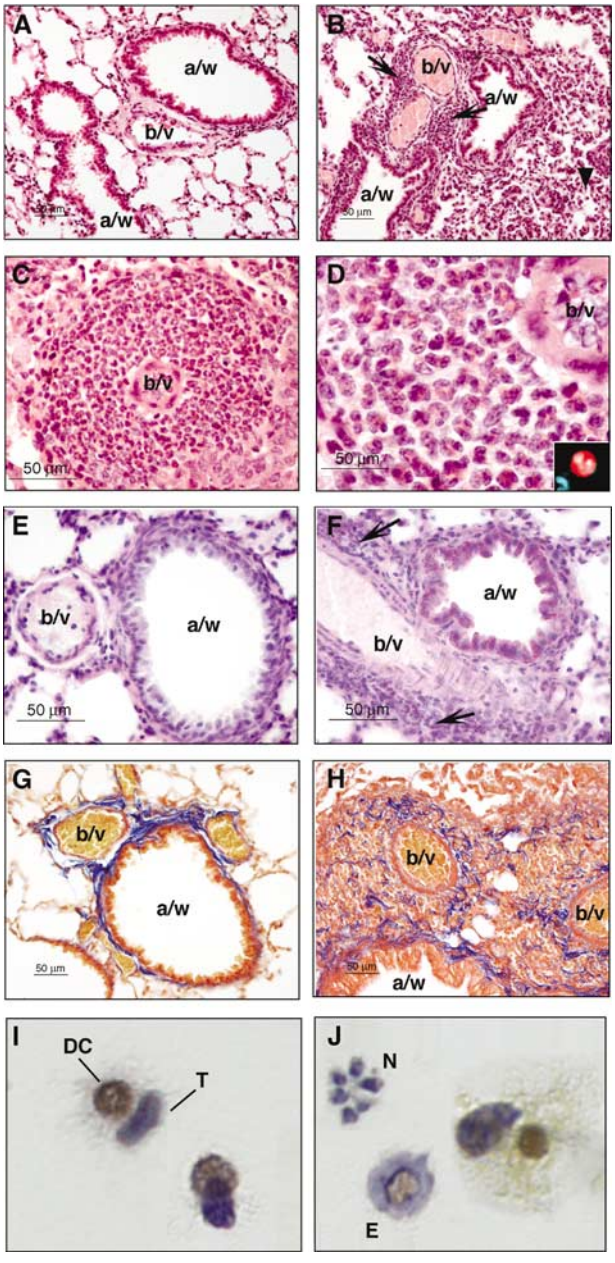

Figure 1 Eosinophil infiltration, mucus hypersecretion and signs of airway remodeling in the lungs of Runx3 KO mice. (**A**) Normal lungs in WT mice showing airways and blood vessels surrounded by alveoli (× 20, HE) (a/w: airway; b/v: blood vessel). (**B**) Lungs in KO mice. The arrows denote infiltrating inflammatory cells, predominantly eosinophils, which accumulate in the interstitium around blood vessels and airways. A mild hypercellularity of the alveoli and alveolar septae denoted by arrowhead is seen in the low right-hand side of the field (× 20, HE). (**C**) A thick eosinophilic perivascular cuff in a KO mouse (× 40, HE). (**D**) High-power view of an area in (C). Eosinophils have eosinophilic cytoplasmic granules and lobed nuclei. The perivascular infiltrate is purely eosinophilic (× 100, HE). The inset at the right-hand corner depicts high-power (× 100) phenol red- and DAPI-stained eosinophils. Phenol red stains the cytoplasm bright red and the lobed nucleus stained with DAPI. (**E**, **F**) WT and KO lungs stained with periodic acid Schiff (PAS), which stains mucus in purple. (E) PAS-positive material is not present in WT (PAS × 40). (F) In the KO, wispy PAS-positive material is observed in the cytoplasm of epithelial cells lining a small caliber airway. Arrows point to clusters of infiltrating inflammatory cells (PAS × 40). (**G**) WT lung stained with Masson's trichrome (MT), which stains collagen fibers in blue. A small amount of collagen is present in the interstitium surrounding blood vessels and airways. Collagen fibers are concentrated around blood vessels and in the region where blood vessels and airways are in apposition (MT × 20). (**H**) KO lung stained with MT. Collagen fibers are deposited in a disorganized manner among clusters of infiltrating inflammatory cells indicating airway remodeling (MT × 20). (**I**, **J**) Runx3 is highly expressed in activated DC from BAL of OVA-challenged WT mice. Experimental acute asthma was induced in WT Balb/C mice. BAL cells immunostained with anti-Runx3 antibodies. (I) Conjugates of DC and T cells; only DC show nuclear staining of Runx3 (brown), whereas T cells are stained only by the hematoxylin counter-stain (blue). (J) Eosinophils (E) and neutrophils (N) are not stained with anti-Runx3 antibodies.

remodeling. No differences between ICR and MF1 backgrounds were observed in onset or severity of the airway inflammation. However, the nonuniform incidence of the lesions may be attributed to the variable genetic backgrounds of the mice (Whitehead *et al*, 2003). Necropsies of older KO mice (2- to 16-month-old) rarely revealed cases of eosinophilic pneumonia (2/12), indicating that the inflammatory infiltration is transient.

Analysis of bronchoalveolar lavages of WT and Runx3 KO mice

The eosinophilic lung inflammation in the KO mice led us to examine the cellular content of bronchoalveolar lavages (BAL) from Runx3 KO and WT mice. Total cell counts revealed a significant increase of cells in KO compared to WT BAL ($1.1 \pm 0.18 \times 10^6$ versus $0.2 \pm 0.09 \times 10^6$ cells/BAL, respectively, $n = 6$, $P = 0.0016$). Moreover, BAL composition analysis showed a marked preponderance of eosinophils in the KO compared to WT littermates ($28.6 \pm 9.1\%$ versus $1.16 \pm 0.4\%$, respectively, $n = 6$, $P = 0.027$). This alveolar eosinophilia was associated, in young (8–11 weeks) KO mice, with increased levels of BAL fluid IL-5 (14.43 ± 8.4 pg/g weight in KO compared to 0.46 ± 0.19 pg/g weight in WT littermates; $P = 0.05$). In older (>14 weeks) mice, IL-5 levels in KO and WT were similar.

In search for the cause of the eosinophilic infiltration in the KO mice, we used an experimental, ovalbumin (OVA)-induced acute asthma model (Topilski *et al*, 2002) to identify Runx3-expressing cells in the alveolar space of the treated animals. WT mice sensitized by OVA were subjected to OVA inhalation and BAL cells were isolated and analyzed for Runx3 expression (Figure 1I and J). BAL of the OVA-treated mice, but not untreated controls, contained abundant conjugates of large mononuclear phagocytes and T cells, which were identified as $CD4^+$ T cells by FACS analysis (not shown). Significantly, within each conjugate, Runx3 expression was detected only in the mononuclear phagocyte; the T cell was negative, as were BAL eosinophils and neutrophils (Figure 1J). Thus, upon allergic sensitization, alveolar DC express high levels of Runx3. This could argue for an intrinsic function of Runx3 in these cells and its involvement in the etiology of the OVA-induced lung eosinophilia. Consistent with this thesis is the fact that when Runx3 is lost, the KO mice develop spontaneous lung eosinophilic inflammation.

In steady state, the murine lung alveolar space is populated by alveolar MØ, which notably coexpress the MØ marker F4/80 and the DC marker CD11c (Figure 2A) and are further characterized by high autofluorescence (Vermaelen *et al*, 2001). Alveolar MØ are poor T-cell stimulators and are believed to be under constant immunosuppression by cytokines such as IL-10 (Holt, 2000). More recently, an additional $F4/80^+/CD11c^+/CD11b^+$ mononuclear phagocyte subset was described, which represents a small population in the resting lung, but accumulates in inflammation (Julia *et al*, 2002). These so-called alveolar DC are potent APC and have a sustained allergen presentation capacity (Julia *et al*, 2002).

To further define the alveolar Runx3-expressing phagocytes, BAL DC/MØ populations of untreated WT and KO mice were studied by flow cytometry. Analysis of KO BAL revealed a striking elevation of the $F4/80^+/CD11c^+/CD11b^+$ subset of alveolar DC as compared to WT BAL (Figure 2B). Furthermore, $CD11c^+$ BAL cells in the KO mice were characterized by increased expression of MHC II (Figure 2C). Compared to WT DC, Runx3 KO BAL DC also displayed a remarkable increase in the expression of OX40L (Figure 2D), a costimulatory molecule shown to play a critical role in the development of allergic lung inflammation (Akbari *et al*, 2003). Significantly, OX40L was markedly elevated on the $CD11c^+/CD11b^+$ subset of alveolar KO DC (Figure 2D).

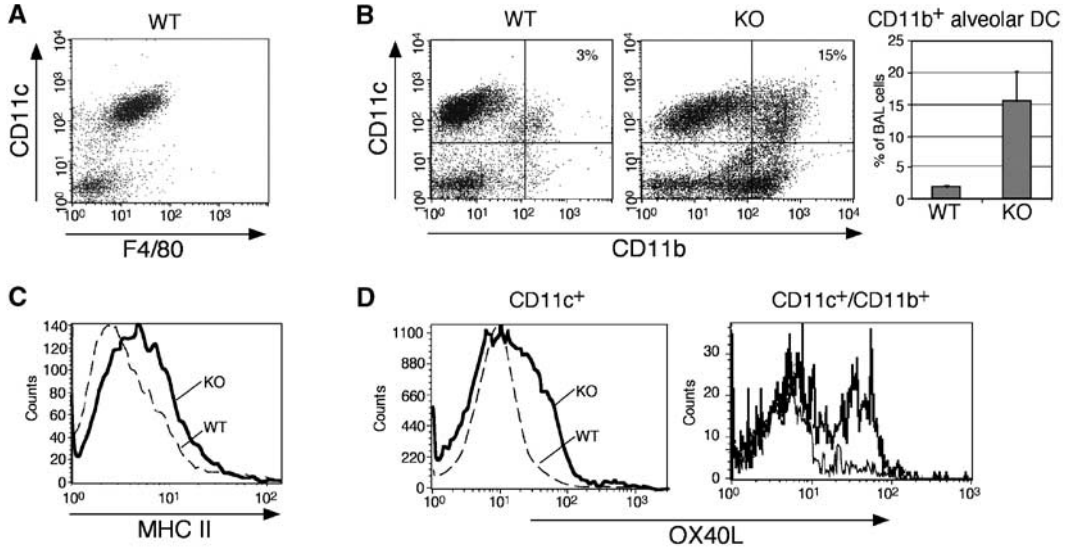

Figure 2 The $F4/80/CD11c^+/CD11b^+/OX40L$ subset of alveolar DC is significantly elevated in the BAL of Runx3 KO mice. Lavage fluid cells were stained with anti-CD11c, anti-CD11b, anti-F4/80, anti-OX40L and anti-MHC II, and analyzed by FACS. (**A**) Most of the $CD11c^+$ alveolar cells also expressed F4/80. (**B**) KO $CD11c^+/CD11b^+$ subset was elevated (from 3 ± 1 to $15 \pm 5\%$, $n = 4$; $P = 0.04$). (**C**, **D**) KO $CD11c^+$ cells also express higher MHC II and OX40L compared to WT. OX40L is mainly elevated in the KO $CD11c^+/CD11b^+$ subset as shown by the histogram on the right.

To examine the response of Runx3 KO and WT mice to aerosol inhalation, mice were challenged with suboptimal doses of OVA. A marked increase in the alveolar DC subset was observed in KO BAL compared to WT ($0.58 \times 10^6 \pm 0.1$ KO versus $0.035 \times 10^6 \pm 0.01$ WT, $n = 4$, $P = 0.009$) along with a two-fold increase in KO BAL eosinophils (not shown). Together, the data demonstrate that Runx3 deficiency results in the accumulation of an $F4/80^+/CD11c^+/CD11b^+/OX40L^{high}$ subset of alveolar DC, which may be responsible for the observed eosinophilic lung inflammation in the Runx3 KO mice.

Induction of Runx3 expression during DC maturation

Expression of Runx3 in lung DC led us to examine its expression in other DC populations and we therefore generated DC from bone marrow (BM) (Lutz *et al*, 2000) (Figure 3A). The nonadherent fraction of WT bone marrow-derived dendritic cell (BMDC) culture consisted at day 7 of immature DC and granulocytes, and at days 11–14 of immature and spontaneously matured DC (~66 and ~33%, respectively). Runx3 protein was barely detected at day 7, but readily detected when mature DC arose (Figure 3B and D). More convincingly, when LPS-treated BMDC cultures were sorted by FACS into mature and immature populations (R2 and R3 in Figure 3A, respectively), collected onto glass slides and immunostained with anti-Runx3 Ab, expression was clearly detected in mature, but was quite faint in immature DC (Figure 3C). Time-course analysis of *Runx3* expression in LPS-treated WT BMDC shows low basal expression level in the first hours after LPS addition and gradual increase thereafter (Figure 3D).

Of note, in mature WT DC three Runx3 protein bands were detected (Figure 3B): two known bands of ~48 and 46 kDa that correspond to the full-length Runx3 proteins (Levanon *et al*, 1994; Shi and Stavnezer, 1998; Le *et al*, 1999; Bangsow *et al*, 2001), and a band of ~33 kDa. Further analysis of this Runx3 p33 product is presented in Supplementary data and Supplementary Figure S1.

To assess Runx3 expression during *in vivo* DC maturation, we took advantage of a mouse strain ($CX_3CR1^{+/GFP}$), in which splenic DC are homogenously green fluorescent labeled (Jung *et al*, 2000). Consistent with the fact that the majority of murine splenic DC are immature and located in the marginal zones (MZ) (Steinman *et al*, 1997), most green fluorescent DC in the $CX_3CR1^{+/GFP}$ mice are found surrounding the white pulp. Upon LPS injection, these DC migrate from the periphery to the central periarteriolar lymphoid sheath (PALS): the T-cell zone (Jung *et al*, 2000). DC migration and function (IL-12 production) are unimpaired in $CX_3CR1^{+/GFP}$ mice (Jung *et al*, 2000).

$CX_3CR1^{+/GFP}$ mice were injected with LPS, sacrificed 6 h later and cryosections of paraformaldehyde-fixed spleens were stained for Runx3 (Figure 3E). Runx3 protein was barely detected in the MZ, consistent with the low levels of Runx3 expression in immature DC, whereas many GFP-positive and -negative cells in the PALS expressed Runx3 (Figure 3E). These Runx3-expressing PALS cells represent both GFP^-/T cells and GFP^+/mature DC. Taken together, the results of Runx3 expression in sorted mature versus immature BMDC and splenic DC *in situ* studies demonstrate that Runx3 is upregulated in DC during maturation.

Runx3 KO DC display enhanced maturation and increased potency to stimulate T cells

Lack of Runx3 is associated with an accumulation of mature DC in BAL of KO mice. We therefore assessed the function of Runx3 in DC maturation. Density gradient-enriched splenic DC were cultured overnight with maturation-inducing reagents and analyzed by FACS (Figure 4A). High concentration of LPS (1 μg/ml) induced maturation of WT DC, reflected in elevated surface expression levels of MHC II and CD86 (Figure 4B and C). LPS-induced maturation was significantly enhanced in KO DC (Figure 4B and C). Of note, KO DC matured even at suboptimal LPS concentrations (100 ng/ml), which did not affect WT DC (Figure 4D). Enhanced maturation, both spontaneous and in response to LPS, was also found in KO BMDC (Supplementary Figure S2). Significantly, this enhanced maturation cannot be explained by upregulation of the toll-like receptors (TLR) 2 and 4, known to mediate responsiveness to LPS as the expression level of TLR2 and TLR4 in KO and WT BMDC was similar (Supplementary Figure S2). Moreover, experiments using other DC maturation stimuli (TNFα and anti-CD40 antibodies) gave similar results (data not shown).

Contrary to immature DC, mature DC are powerful T-cell stimulators (Steinman, 1999). We addressed whether enhanced maturation of Runx3 KO DC results in increased efficacy to prime T cells by using a syngeneic oxidative mitogenesis assay (Austyn *et al*, 1983) and a mixed leukocyte reaction (MLR). In both assays, Runx3 KO DC were significantly more efficient stimulators of $CD4^+$ T-cell proliferation compared to WT DC (Figure 4E). Taken together, these data indicate a critical role for Runx3 in DC differentiation and function.

Impaired TGF-β signaling in Runx3 KO DC

In vitro studies have previously shown that Runx3 participates in TGF-β-directed IgA class switching (Shi and Stavnezer, 1998). More recently, Runx3 was implicated in TGF-β-mediated growth inhibition and apoptosis of stomach epithelium (Li *et al*, 2002; Ito and Miyazono, 2003). In the DC compartment, TGF-β has a dual function: it is required for the development of the epidermal LC (Borkowski *et al*, 1996), and acts as a DC maturation inhibitor (Yamaguchi *et al*, 1997).

To investigate the effect of Runx3 deficiency on TGF-β signaling in DC, we assessed LC development in Runx3 KO mice. Skin epidermis of KO mice completely lacked LC (Figure 5A), whereas abundance of dendritic epidermal T cells was similar to WT skin (R3 versus R2 in Figure 5B). It was recently reported that mice deficient for Id2, a TGF-β-induced inhibitor of helix–loop–helix transcription factors, also lack LC (Hacker *et al*, 2003). Analysis of *Id2* expression in TGF-β-treated BMDC revealed similar levels in WT and KO DC (Figure 5C). Thus, the absence of LC in Runx3 KO is not due to lack of Id2. Of note, contrary to Id2 expression, which was greatly induced by TGF-β (Figure 5C), expression of Runx3 in BMDC was not affected by TGF-β (Supplementary Figure S1).

Next we investigated the effect of TGF-β on maturation of Runx3 KO and WT DC. As shown in Figure 5D, TGF-β inhibited the LPS-induced maturation of WT BMDC, but strikingly failed to do so in KO BMDC. Even after short (4 h) LPS induction, TGF-β significantly inhibited the matura-

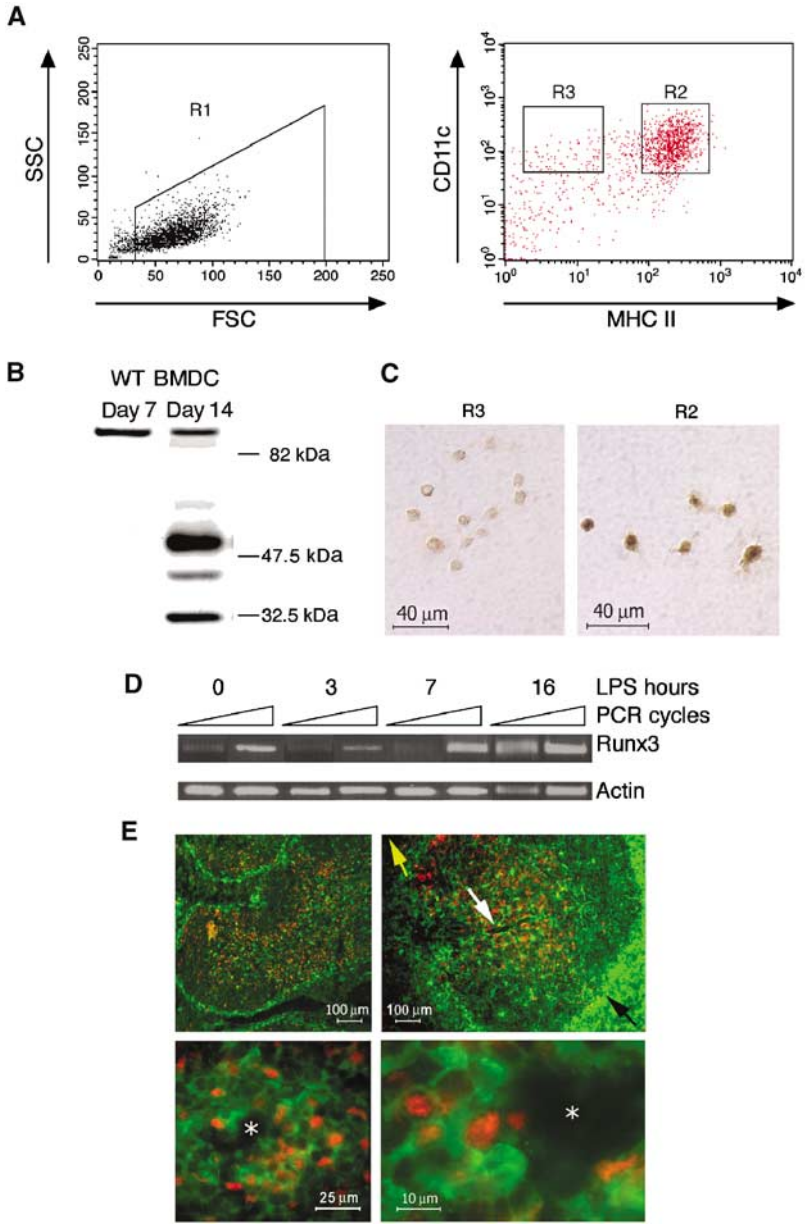

Figure 3 Runx3 expression is induced upon maturation of BMDC. (**A**) Runx3 expression in sorted WT DC. Day 11 BMDC treated with LPS (1 μg/ml), stained with anti-CD11c and anti-MHC II and analyzed by FACS. DC were gated as high forward scatter cells (R1) and sorted into $CD11c^+$ mature, MHC II high (R2) and immature, MHC II low (R3), respectively. (**B**) Expression of Runx3 in spontaneously matured WT BMDC. Western blot of proteins from immature (7 days) and matured (14 days) cultured WT BMDC using anti-Runx3 Ab. Note the similar intensity of the 85 kDa nonspecific protein band in immature and mature BMDC. (**C**) Immunostaining of Runx3 in FACS-sorted mature BMDC. R2 or R3 cells (4×10^3) were collected onto slides and immunostained with anti-Runx3 Ab. (**D**) Expression of *Runx3* during BMDC maturation. Day 7 immature WT BMDC were treated with LPS (1 μg/ml), and at the indicated time points RNA was extracted and analyzed by semiquantitative RT–PCR. Equal amounts of cDNA (compared to actin) were used for PCR and the number of cycles was preoptimized. *Runx3* was determined at 26 and 28 cycles (yielding a 654 bp fragment) and actin at 15 and 16 cycles (439 bp fragment) with primers indicated in Supplementary Figure S1. (**E**) In the spleen, Runx3 protein is detected in mature periarteriolar lymphoid sheath DC. Cryosections of spleens of $CX_3CR1^{+/GFP}$ mice 6 h after injection of LPS (80 μg), stained with anti-GFP and anti-Runx3 Ab are shown. Upper panels are at low magnification showing the absence of Runx3 staining (red nuclear staining) in MZ immature DC (green GFP-positive cytoplasmic staining). Lower panels are at higher magnification showing Runx3 expression in mature DC located in the periarteriolar lymphoid sheaths. The yellow arrow designates the splenic red pulp, while the black designates the MZ of the white pulp. The white arrow designates the PALS surrounding the central arteriole (white asterisk).

tion of WT but not KO BMDC (Supplementary Figure S2B). The results indicate that Runx3 functions as part of the TGF-β signaling pathway in DC. Significantly, expression of other components of the TGF-β cascade, including TGF-β type I and II receptors (TβR-I and TβR-II) and TGF-β signal transducers Smad2 and Smad3, was unchanged in KO BMDC, as was the TGF-β-mediated phosphorylation of Smad2 (Supplementary Figure S3). Interestingly, the role of Runx3 in TGF-β signaling extends to other Runx3-expressing cells, as Runx3 KO splenocytes showed impaired TGF-β-directed IgA class switching (Supplementary data and Supplementary Figure S4).

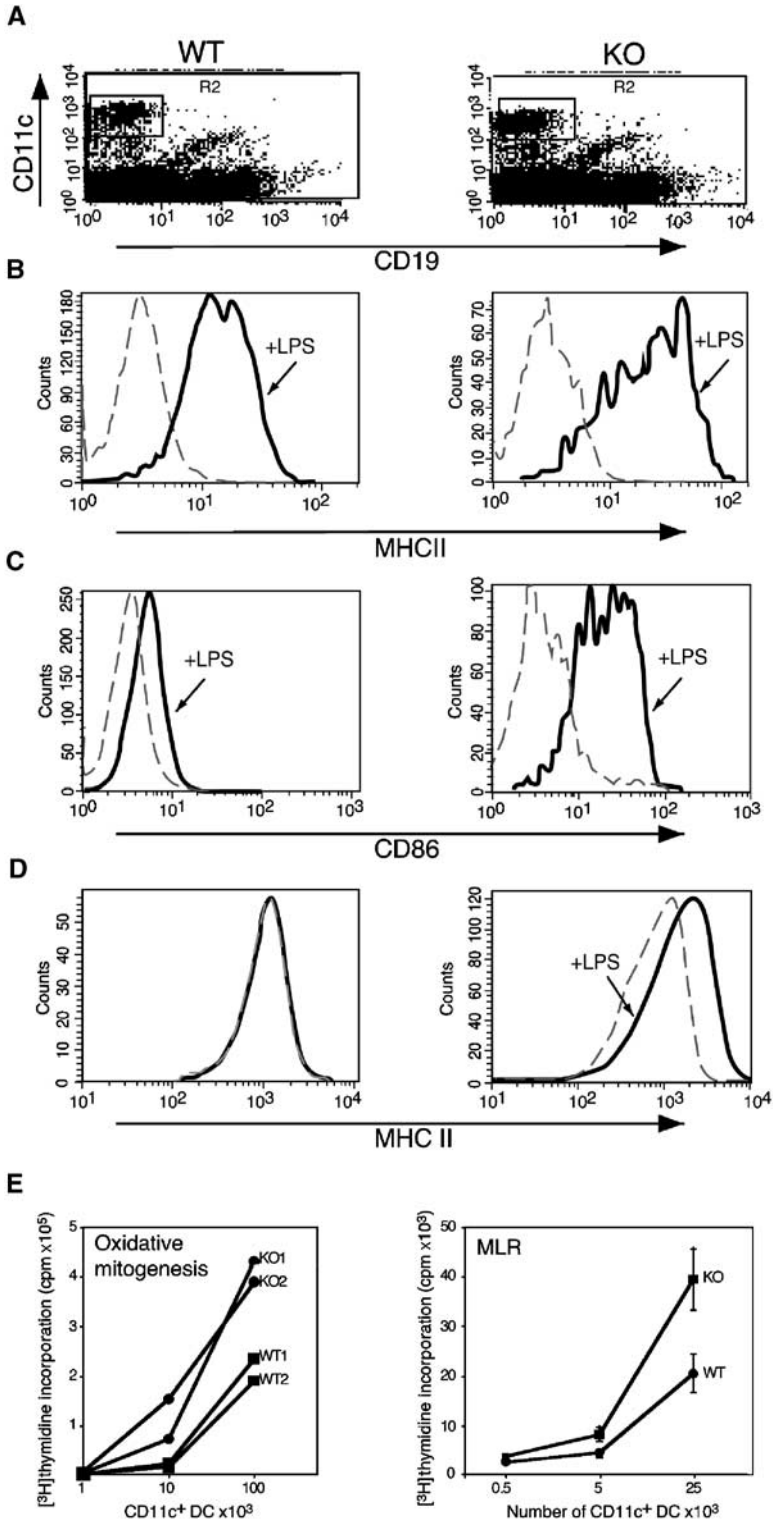

Figure 4 Runx3 KO DC display enhanced maturation and increased ability to stimulate T-cell proliferation. Splenic DC of Runx3 KO and WT mice were cultured overnight without or with LPS (1 μg/ml), stained and analyzed by FACS (A–C). (**A**) $CD11c^+/CD19^-$ KO or WT DC were gated (R2). (**B**, **C**) Expression of MHC II and CD86, respectively, in untreated (dotted line) and LPS-treated (solid line) WT and KO DC was measured. (**D**) Splenic DC were cultured in a suboptimal concentration of LPS (100 ng/ml) and analyzed for MHC II. Maturation was observed only in KO DC. (**E**) Syngeneic oxidative mitogenesis (left panel): Increasing numbers of WT and KO DC were incubated for 24 h with 3×10^5 purified sodium periodate-treated $CD4^+$ T cells of the same mouse. MLR (right panel): DC were incubated for 64 h with 1×10^5 purified $CD4^+$ T cells from each of the three WT strains C57/BL, BALB/C and SJL and thymidine incorporation was determined (Austyn *et al*, 1983). The results of oxidative mitogenesis are presented as cpm per $CD11c^+$ DC (determined by FACS analysis). One experiment out of two with similar results is shown. MLR data represent the average at each point of (Austyn *et al*, 1983) thymidine incorporated by T cells of the three WT mouse strains. At the lower DC/T-cell ratio in the oxidative mitogenesis assay, only the KO DC induced T-cell proliferation.

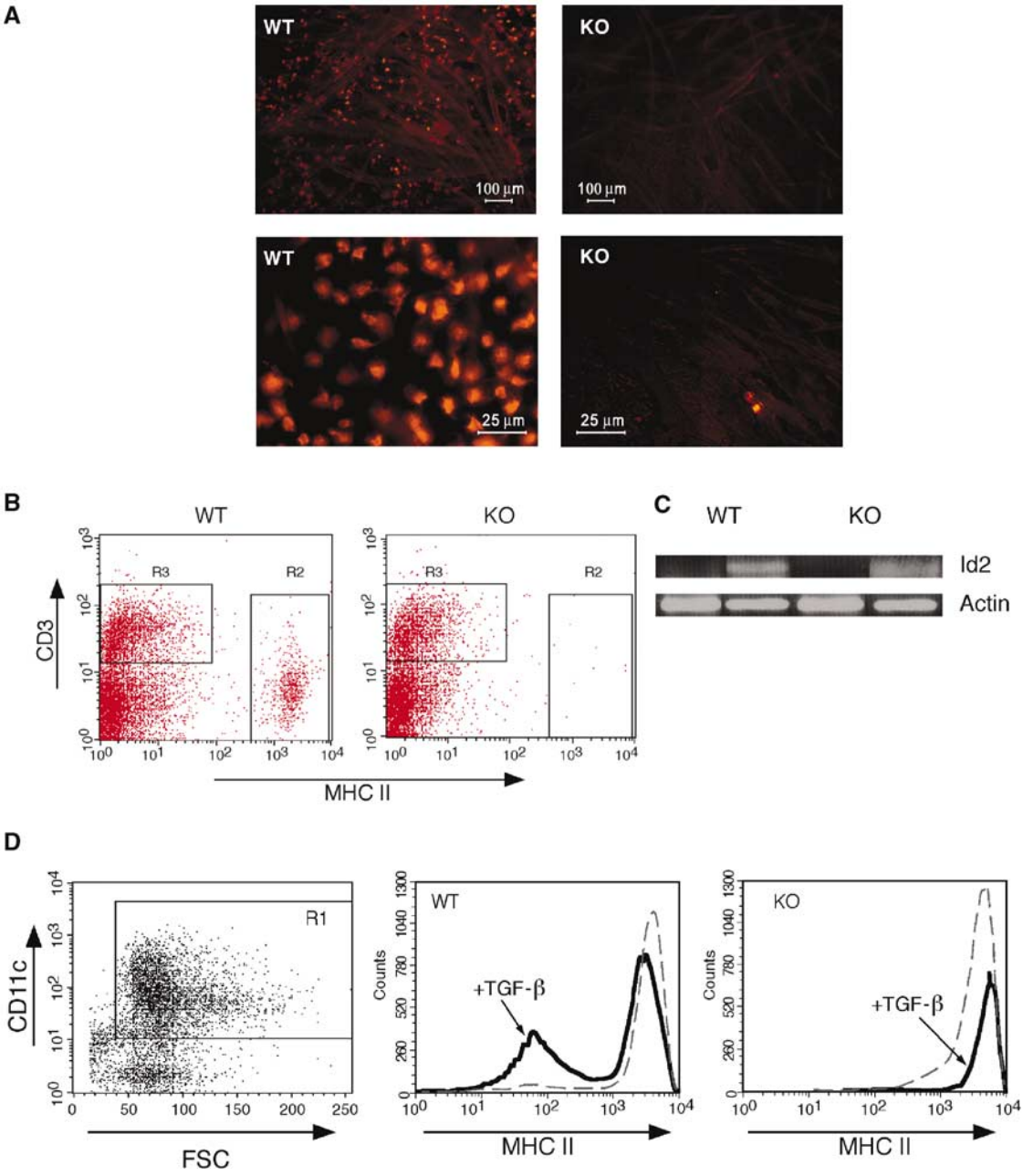

Figure 5 Loss of TGF-β-mediated functions in Runx3 KO DC compartment. (**A**) Epidermal sheaths were prepared and stained with PE-conjugated anti-MHC II Ab to detect LC. LC are seen in the WT preparation, but are absent in the KO. Upper and lower panels depict low and high magnifications, respectively. (**B**) Single-cell suspension derived from epidermal sheaths of KO and WT mice, stained with MHC II and CD3 Ab and analyzed by FACS. T-cell populations (R3) were similar in WT and KO, whereas LC (R2) are absent in the KO mice. (**C**) TGF-β-induced expression of *Id2* in WT and KO BMDC. WT and Runx3 KO BMDC were grown in the presence or absence of TGF-β (10 ng/ml) and at day 7 were treated for 16 h with LPS (1 μg/ml). *Id2* was determined by RT–PCR at 35 cycles with the primers F, AGCATCCCCCAGAACAAGAAGGTG; R, ATCGCTTGCCCAGGTGTCGTTCT, yielding a fragment of 441 bp and compared to actin at 17 cycles with the primers indicated in Supplementary Figure S1. (**D**) Runx3 KO and WT BMDC were incubated with GM-CSF with or without TGF-β (10 ng/ml). Day 7 cells (10^6 cells/ml) were cultured overnight with 1 μg/ml LPS, collected and stained with anti-CD11c and anti-MHC II antibodies. KO or WT DC were gated as CD11c+ cells (R1) and assessed for expression of MHC II. TGF-β inhibited a significant part of the LPS-induced maturation reflected in an increase of MHC II^{low} cells, whereas maturation of KO BMDC was not affected by TGF-β.

Altered expression pattern of β2-integrins in Runx3 KO DC

The implication of RUNX3 in the regulation of lymphoid- and myeloid-specific activity of the CD11a promoter (Puig-Kroger *et al*, 2003 and references therein) led us to test whether Runx3 deficiency affects DC β2-integrin expression. Splenic DC of Runx3 KO and WT littermates were analyzed by FACS (Figure 6A). KO DC displayed a marked reduction in CD11c, an elevation of CD11b and a small increase of CD11a expression, as compared to WT DC. Expression of CD11c was also significantly reduced on DC isolated from Runx3 KO mesenteric lymph nodes and Peyer's patches as well as on Runx3 KO BMDC (data not shown). Of note, expression levels of the β-chain (CD18), common to all three β2-integrins, were not

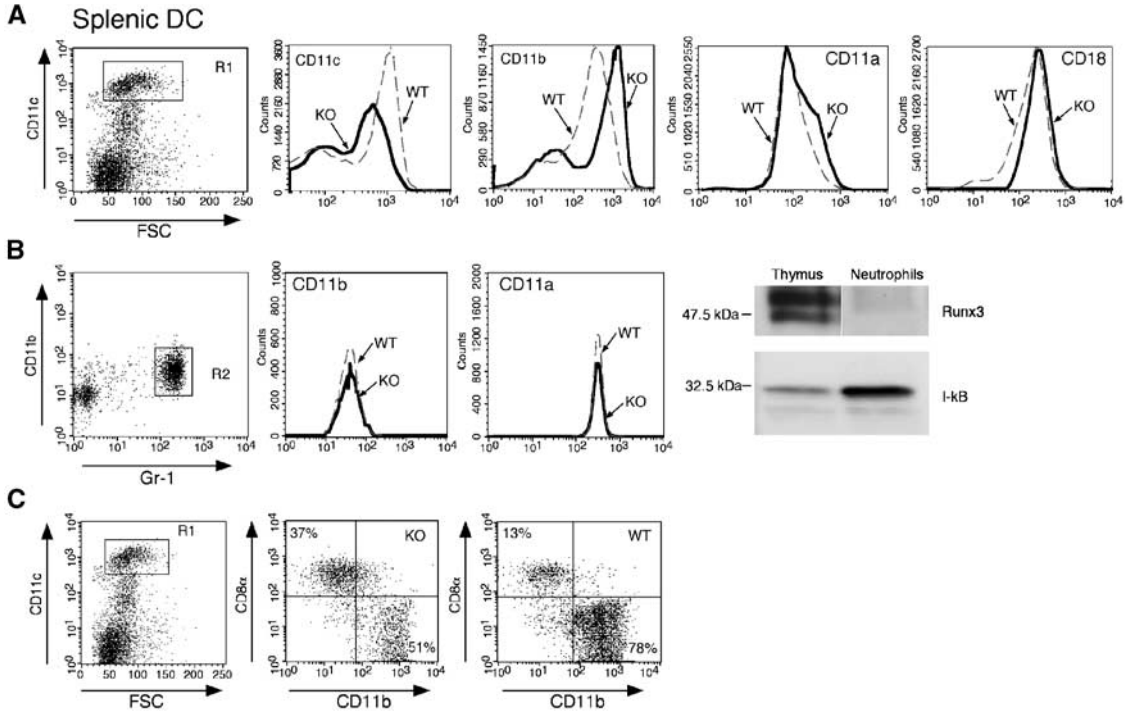

Figure 6 Altered expression of β2-integrins in Runx3 KO mice. (**A**) WT and Runx3 KO splenic DC analyzed by FACS using anti-CD11c, anti-CD11b and anti-CD11a antibodies. Cells were gated as high forward scatter/CD11c^{high} population (R1) and assessed for expression of the three β2-integrins. Solid and dotted lines represent Runx3 KO and WT littermates, respectively. CD11a and CD11b were elevated in the KO compared to WT, whereas CD11c decreased. Expression of the β2-integrins common β-chain (CD18) in WT and KO DC was similar. (**B**) Normal expression of β2-integrins in Runx3 KO neutrophils. Peripheral blood leukocytes (PBL) of Runx3 KO and WT mice stained with anti-Gr-1, anti-CD11b and anti-CD11a antibodies and neutrophils gated as high side scatter/CD11b$^+$/Gr-1$^+$ cells (R2). Expression of CD11b and CD11a in WT (dotted line) and KO (solid line) was monitored. Peritoneal lavage neutrophils were obtained following induction of peritonitis and analyzed for Runx3 by Western blots in parallel with proteins of WT thymus. Blots were reacted with anti-Runx3 and anti-I-kB Ab. (**C**) The CD8$^+$ population of splenic DC is elevated in Runx3 KO mice. Splenic DC of Runx3 KO and WT littermates were reacted with anti-CD11c, anti-CD11b and anti-CD8α antibodies. High forward scatter/CD11c+ population (R1) of DC was gated and assessed for CD11b and CD8α. Percentage of CD8$^+$/CD11b$^-$ DC in the KO was elevated and that of CD8$^-$/CD11b$^+$ reduced as compared to WT.

affected by the loss of Runx3 (Figure 6A). These data indicate that Runx3 is directly involved in regulating coordinated β2-integrin expression. Consistent with this conclusion, expression of β2-integrins on neutrophils, which do not express Runx3, was similar in both WT and KO (Figure 6B).

Splenic DC fall into two distinct populations, defined by differential expression of CD11b and CD8α. Analysis of splenocytes revealed a significant preponderance of CD8$^+$/CD11b$^-$ DC in KO compared to WT (35.0 ± 4.1 versus $15.5 \pm 2.1\%$, $n=4$; $P=0.02$), along with a decrease in CD8$^-$/CD11b$^+$ DC (55.3 ± 4.9 versus $68.7 \pm 0.9\%$, $n=4$; $P=0.04$) (Figure 6C). This altered DC population balance adds to the changes in the KO DC compartment and may contribute to the increased inflammatory response in Runx3 KO mice.

Discussion

One of the challenges encountered by the immune system is to distinguish between pathogenic and innocuous antigens and respond accordingly by developing active immunity or tolerance, respectively. Allergic asthma is a disease characterized by a Th2 immune reaction and pulmonary eosinophilic inflammation in response to inhaled antigens. Despite considerable evidence suggesting that T lymphocytes play a pivotal role in the pathogenesis of asthma, the molecular signals that direct the differentiation of naïve T cells into pathogenic Th2 cytokine-producing cells in response to inhaled antigens are not well understood (Keane-Myers *et al*, 1998). Recent studies point to a primary role of DC in regulating *in vivo* allergic responses (Keane-Myers *et al*, 1998; Lambrecht *et al*, 2000).

Here we show that Runx3 KO mice develop pulmonary eosinophilic inflammation associated with airway remodeling and mucus hypersecretion. This eosinophilic inflammation occurs spontaneously without intentional exogenous challenge and is accompanied by an increase in the Th2 cytokine IL-5. Interestingly, however, the inflammation disappears after several weeks without any treatment, and is very rarely detected in KO mice older than 12 weeks. Morphologically, lung lesions of Runx3 KO mice are reminiscent of the human conditions asthma (Cotran *et al*, 1999) and eosinophilic bronchitis (Brightling *et al*, 2003).

Using an experimental asthma model, we found that out of the cell types participating in lung inflammation response, that is, granulocytes, lymphocytes and MØ/DC, only the latter express Runx3. Interestingly, Runx3 protein is barely detected in immature DC, but is highly expressed in mature DC. In the spleen, Runx3 expression is mainly in mature PALS DC. These results are in good agreement with DNA microarray data (Huang *et al*, 2001) showing increased transient expression of *RUNX3* mRNA upon maturation of human

monocyte-derived DC. It is thus conceivable that Runx3 functions in DC to restrain spontaneous maturation, but through which signaling pathway?

Members of the TGF-β family control growth, differentiation and apoptosis of cells, and have important functions in hematopoiesis and embryogenesis (Massague *et al*, 2000). Runx family members have been implicated in various TGF-β-mediated events (Ito and Miyazono, 2003). Notably, Runx3 was shown to mediate TGF-β signaling in gastric epithelial cells, as Runx3 KO mice exhibited hyperplasia of gastric epithelium attributed to lower sensitivity of these cells to TGF-β signals (Li *et al*, 2002; Ito and Miyazono, 2003). In DC, TGF-β was reported to exert a pronounced inhibitory effect on maturation (Yamaguchi *et al*, 1997). TGF-β is also required for *in vitro* and *in vivo* development of epidermal LC (Borkowski *et al*, 1996; Jaksits *et al*, 1999). Here we show that Runx3 KO BMDC do not respond to TGF-β-induced maturation inhibition, even though the expression of other known components of the TGF-β signaling pathway such as TβR-I and TβR-II as well as Smad2 and Smad3 were unaffected in KO DC. Moreover, Runx3 KO mice lack epidermal LC. Taken together, these findings establish a role for Runx3 in the TGF-β signaling cascade in DC. Mice deficient for Id2 also lack LC (Hacker *et al*, 2003). However, analysis of Id2 expression in the KO DC demonstrated that Runx3 does not act as an upstream regulator of Id2 in TGF-β-dependent development of LC.

RUNX/AML family members and in particular Runx3/AML2 cooperate with Smads in TGF-β-mediated transcriptional activation of the GL Ig α promoter in various cell lines and in murine splenic B cells (Shi and Stavnezer, 1998). Interestingly, using isolated splenocytes from Runx3 KO and WT mice, we found that TGF-β-dependent class switching to IgA was abrogated in the KO cells (Supplementary data), providing another *in vivo* indication of Runx3 function as a mediator of TGF-β signaling.

In the lungs of the KO mice, lack of response to TGF-β and the resulting unrestrained maturation of DC are associated with an accumulation of alveolar DC. This DC subset, which is barely detectable in the lungs of WT mice, was recently identified as a potent APC, with a sustained allergen presentation capacity (Julia *et al*, 2002). Significantly, Runx3 KO alveolar DC also expressed higher levels of the costimulatory molecule OX40L, known to play a role in the development of allergic inflammation in mice (Akbari *et al*, 2003). Not only are Runx3 KO DC resistant to TGF-β-mediated maturation attenuation, they also over-respond to various maturation stimuli such as LPS, TNFα and CD40 engagement. Mature KO DC appeared to be highly potent APC with increased expression of MHC class II and T-cell costimulatory molecules (CD80, CD86 and OX40L). Indeed, when tested in syngeneic and allogenic MLRs, Runx3 KO DC displayed a significantly higher potency to stimulate T cells as compared to WT DC. Together, these occurrences suggest a scenario in which Runx3 KO DC that over-react to innocuous airborne antigens activate T cells, culminating in enhanced recruitment of eosinophils to the lungs of KO mice.

The accelerated maturation of Runx3 KO DC was also associated with aberrant expression of β2-integrins, even though the expression of the common CD18 β-chain was unchanged. Intriguingly, while the expression of CD11c significantly decreased in the KO, the expression of CD11b and CD11a increased. This opposite effects on the expression of the β2-integrin α-chains could have resulted from the bifunctional nature of Runx3, which can act both as an activator or a repressor of target gene transcription, through recruitment of the corepressor Gro/TLE (Levanon *et al*, 1998). As the β2-integrins play an important role in DC maturation and extravasation (De La Rosa *et al*, 2003), changes in the β2-integrin expression profile in the KO DC could contribute to the etiology of lung inflammation. This conclusion is supported by the finding that CD18-deficient mice show defective DC migration to the lungs (Schneeberger *et al*, 2000).

In the spleens of Runx3 KO mice, we observed a significant preponderance of $CD11b^-/CD8^+$ DC, along with a decrease of $CD11b^+/CD8^-$ DC. Although specific differential roles of these DC subset have not been defined, $CD8^+$ and $CD8^-$ DC have been associated with Th1- and Th2-biased responses, respectively (Shortman and Liu, 2002). The population imbalance of splenic DC in Runx3 KO mice may therefore contribute to the increased inflammatory response observed in Runx3 KO mice.

The data presented here provide evidence for the importance of Runx3 as a component of the TGF-β signaling cascade in DC. When Runx3 is lost, epidermal LC are absent and KO DC display accelerated maturation due to lack of responsiveness to TGF-β and over-responsiveness to maturation stimuli. Furthermore, KO DC exhibit aberrant expression of β2-integrins and population imbalances in the spleen. In the lungs of the KO mice, a unique subset of alveolar DC is increased. The accumulation of these DC and their enhanced T-cell stimulatory capacity might reflect an over-response to otherwise innocuous airborne antigens, possibly due to lack of responsiveness to locally secreted TGF-β. This may result in activation of T cells, which elicit enhanced recruitment of eosinophils to the lungs, leading to inflammation, mucus hypersecretion and airway remodeling in Runx3 KO mice.

RUNX3 resides on human chromosome 1p36.1 (Levanon *et al*, 1994), a region recently identified to contain candidate susceptibility genes for asthma and hypersensitivity against environmental antigens (Haagerup *et al*, 2002). It will therefore be interesting to examine whether in humans, mutations in *RUNX3* are associated with susceptibility to asthma.

Materials and methods

Mice strains and treatments

Runx3 KO mice were generated as described previously (Levanon *et al*, 2002) and bred on ICR and MF1 background. KO mice and WT littermates of both backgrounds were used for the experiments. $CX_3CR1^{+/GFP}$ mice (Jung *et al*, 2000) were kept on C57BL/6 background. Mice were maintained in individually ventilated cages in an SPF facility free of known viral and bacterial pathogens. For BAL, 8- to 9-week-old Runx3 KO and age/sex-matched WT littermate mice were sacrificed by CO_2 asphyxiation, tracheae were cannulated and lungs were washed by gentle infusion of 2–4 aliquots of 1 ml PBS. Experimental acute asthma was induced in C57BL/6 mice as described (Topilski *et al*, 2002). Peritonitis for neutrophil isolation was induced in WT mice by intraperitoneal injection of 3 ml 10% sodium caseinate. Analysis of LC was performed using ear epidermal sheets prepared by splitting the ear and placing its dermal side down in 1% trypsin solution for 45 min at 37°C. Epidermal sheets were peeled off the underlying dermis and subjected to further analysis.

Lung histology

Lungs were inflated with, and immersion fixed in 10% neutral buffered formalin. Tissue was processed routinely, embedded in

paraffin and trimmed at 4 μm. Selected cases were stained with periodic acid Schiff (PAS) and Masson's trichrome. The identity of eosinophils was confirmed using the phenol red staining procedure (Ain *et al*, 2002). Nuclei were counterstained with DAPI.

Bone marrow cultures

BMDC were prepared as described (Lutz *et al*, 2000). Briefly, mice were sacrificed and BM was extracted from femurs and tibias by flushing the shaft with 5 ml RPMI-1640. Red blood cells (RBC) were lysed in 1.66% NH_4Cl, and cells seeded into nontissue culture plates at a density of 1×10^6 cells/ml in medium (RPMI-1640, 10% FCS, 5×10^{-5} M 2-mercapto ethanol, penicillin/streptomycin) containing 10 ng/ml murine recombinant GM-CSF (Peprotech, Rehovot, Israel). The medium was replenished every 3 days and the loosely adherent DC were collected at designated time points and used for further studies. To induce DC maturation, day 7–12 cultures were treated with LPS (0.1–1 μg/ml) and analyzed 1 day later.

Gradient-enriched splenic DC

Spleens were isolated, minced and incubated with 1 mg/ml collagenase (Sigma) for 45 min at 37°C. RBC were lysed and cells resuspended at a density of 5×10^7 cells/ml in a 14.5% Nycodenz solution (Nycomed, Pharma AS diagnostics, Oslo, Norway). Buffer (2 ml) was layered carefully onto 4 ml of Nycodenz cell suspension, centrifuged (1500 $g \times$ 13 min at 4°C) and the low-density cell layer was collected for further experiments.

Flow cytometry and ELISA

Single-cell suspensions were prepared in FACS buffer (PBS, 1 mM EDTA, 1% BSA/0.05% sodium azide). Immunostaining ($1–2 \times 10^6$ cells) was performed in the presence of rat anti-mouse Fc gamma RIII/II receptor (CD16/32; clone 2.4G2, ATCC), by incubating the cells with monoclonal antibodies for 30 min on ice (100 μl per 1×10^6 cells). Flow cytometry was performed with a FACSCalibur (Becton Dickinson, Mountainview, CA) and CellQuest software (Becton Dickinson). Cell sorting was performed with a FACS sorter (Vantage). Staining reagents included CD8-Percp, CD11c APC/PE, CD11b PE/FITC, CD11a/FITC, IA/IE PE, IAb FITC, CD80 FITC, CD86 FITC, streptavidin APC/PE, biotinylated OX40L, CD3 and CD4 (Pharmingen, San Diego, CA). IL-5 levels in BAL were determined using the mouse IL-5 ELISA detection kit (Duoset, Minneapolis, MN).

MLR and syngeneic oxidized T-cell proliferation assays

Cells were obtained from spleen and lymph nodes of Runx3 KO and WT littermate ICR mice as well as from three MHC haplotype-mismatched inbred WT strains (C57/BL/6 ($H2^b$), BALB/C ($H2^d$) and SJL ($H2^s$). $CD4^+$ T cells were isolated by MACS (Miltenyi biotec, Bergish Gladbach, Germany) yielding ~95% pure $CD4^+$ T cells. Syngeneic T cells of KO and WT littermates were oxidized by 15 min incubation on ice in 0.25 mg/ml sodium periodate, as described previously (Austyn *et al*, 1983). Purified $CD4^+$ T cells were incubated at 37°C in a final volume of 0.2 ml, with increasing numbers of splenic Nycodenz density gradient-enriched DC. After 1–3 days (Austyn *et al*, 1983), thymidine (0.05 μCi/μl in oxidative mitogenesis or 0.1 μCi/μl in MLR) was added and incubation at 37°C was continued for 14 and 8 h in oxidative mitogenesis and MLR, respectively. Cells were collected and incorporated radioactivity was determined as described (Woolf *et al*, 2003).

Immunohistochemistry

BMDC ($CD11c^+$) were sorted into mature (MHC II^{high}) and immature (MHC II^{low}) subsets and Runx3 was detected using affinity-purified rabbit anti-RUNX3 antibodies raised against the carboxy half of the protein (Levanon *et al*, 2001a; Woolf *et al*, 2003). For cryostat sections, tissues were fixed with 4% paraformaldehyde to preserve GFP. Sections (12–16 μm) were stained overnight with mouse monoclonal anti-GFP antibodies (clone B34, Babco, Richmond, CA) and rabbit anti-RUNX3 antibodies, washed and reacted for 2 h at room temperature with fluorochrome-labeled secondary antibodies (488 goat anti-mouse and 568 goat anti-rabbit; Molecular Probes, Eugene, OR). Data were acquired by fluorescent and confocal microscopy.

Supplementary data

Supplementary data are available at *The EMBO Journal* Online.

Acknowledgements

We thank Judith Chermesh, Rafi Saka and Shoshana Grossfeled for help in animal husbandry, Dorit Nathan, Tamara Berkuzki, Raya Eilam, Nora Mauerman and Eti Yael for technical assistance, and Ayala Sharp and Eitan Ariel for help in FACS analysis. We are grateful to Peter ten Dijke for his generous gift of antibodies. This work was supported by grants from the Commission of the EU, the Israel Science Foundation, Minerva Foundation Germany and Shapell Family Biomedical Research Foundation at the Weizmann Institute. SJ is an incumbent of the Pauline Recanati Career Development Chair and a Benoziyo Scholar of Molecular Medicine.

References

Ain R, Tash JS, Soares MJ (2002) A simple method for the *in situ* detection of eosinophils. *J Immunol Methods* **260:** 273–278

Akbari O, Stock P, DeKruyff RH, Umetsu DT (2003) Mucosal tolerance and immunity: regulating the development of allergic disease and asthma. *Int Arch Allergy Immunol* **130:** 108–118

Austyn JM, Steinman RM, Weinstein DE, Granelli-Piperno A, Palladino MA (1983) Dendritic cells initiate a two-stage mechanism for T lymphocyte proliferation. *J Exp Med* **157:** 1101–1115

Bae S-C, Takahashi E-i, Zhang YW, Ogawa E, Shigesada K, Namba Y, Satake M, Ito Y (1995) Cloning, mapping and expression of PEBP2aC, a third gene encoding the mammalian *runt* domain. *Gene* **159:** 245–248

Banchereau J, Steinman RM (1998) Dendritic cells and the control of immunity. *Nature* **392:** 245–252

Bangsow C, Rubins N, Glusman G, Bernstein Y, Negreanu V, Goldenberg D, Lotem J, Ben-Asher E, Lancet D, Levanon D, Groner Y (2001) The RUNX3 gene—sequence, structure and regulated expression. *Gene* **279:** 221–232

Ben Aziz-Aloya R, Levanon D, Karn H, Kidron D, Goldenberg D, Lotem J, Polak-Chaklon S, Groner Y (1998) Expression of AML1-d, a short human AML1 isoform, in embryonic stem cells suppresses *in vivo* tumor growth and differentiation. *Cell Death Differ* **5:** 765–773

Borkowski TA, Letterio JJ, Farr AG, Udey MC (1996) A role for endogenous transforming growth factor beta 1 in Langerhans cell biology: the skin of transforming growth factor beta 1 null mice is devoid of epidermal Langerhans cells. *J Exp Med* **184:** 2417–2422

Brightling CE, Symon FA, Birring SS, Bradding P, Wardlaw AJ, Pavord ID (2003) Comparison of airway immunopathology of eosinophilic bronchitis and asthma. *Thorax* **58:** 528–532

Cotran R, Kumar V, Collins T (1999) *Robbins Pathologic Basis of Disease*. Philadelphia: WB Saunders Company

De La Rosa G, Longo N, Rodriguez-Fernandez JL, Puig-Kroger A, Pineda A, Corbi AL, Sanchez-Mateos P (2003) Migration of human blood dendritic cells across endothelial cell monolayers: adhesion molecules and chemokines involved in subset-specific transmigration. *J Leukoc Biol* **73:** 639–649

Geoffroy V, Corral DA, Zhou L, Lee B, Karsenty G (1998) Genomic organization, expression of the human CBFA1 gene, and evidence for an alternative splicing event affecting protein function. *Mamm Genome* **9:** 54–57

Ghozi MC, Bernstein Y, Negreanu V, Levanon D, Groner Y (1996) Expression of the human acute myeloid leukemia gene *AML1* is regulated by two promoter regions. *Proc Natl Acad sci USA* **93:** 1935–1940

Haagerup A, Bjerke T, Schiotz PO, Binderup HG, Dahl R, Kruse TA (2002) Asthma and atopy—a total genome scan for susceptibility genes. *Allergy* **57:** 680–686

Hacker C, Kirsch RD, Ju XS, Hieronymus T, Gust TC, Kuhl C, Jorgas T, Kurz SM, Rose-John S, Yokota Y, Zenke M (2003) Trans-

criptional profiling identifies Id2 function in dendritic cell development. *Nat Immunol* **4:** 380–386

Holt PG (2000) Antigen presentation in the lung. *Am J Respir Crit Care Med* **162:** S151–S156

Huang Q, Liu D, Majewski P, Schulte LC, Korn JM, Young RA, Lander ES, Hacohen N (2001) The plasticity of dendritic cell responses to pathogens and their components. *Science* **294:** 870–875

Inoue K, Ozaki S, Shiga T, Ito K, Masuda T, Okado N, Iseda T, Kawaguchi S, Ogawa M, Bae SC, Yamashita N, Itohara S, Kudo N, Ito Y (2002) Runx3 controls the axonal projection of proprioceptive dorsal root ganglion neurons. *Nat Neurosci* **5:** 946–954

Ito Y (1999) Molecular basis of tissue-specific gene expression mediated by the runt domain transcription factor PEBP2/CBF. *Genes Cells* **4:** 685–696

Ito Y, Miyazono K (2003) RUNX transcription factors as key targets of TGF-beta superfamily signaling. *Curr Opin Genet Dev* **13:** 43–47

Jaksits S, Kriehuber E, Charbonnier AS, Rappersberger K, Stingl G, Maurer D (1999) CD34+ cell-derived CD14+ precursor cells develop into Langerhans cells in a TGF-beta 1-dependent manner. *J Immunol* **163:** 4869–4877

Julia V, Hessel EM, Malherbe L, Glaichenhaus N, O'Garra A, Coffman RL (2002) A restricted subset of dendritic cells captures airborne antigens and remains able to activate specific T cells long after antigen exposure. *Immunity* **16:** 271–283

Jung S, Aliberti J, Graemmel P, Sunshine MJ, Kreutzberg GW, Sher A, Littman DR (2000) Analysis of fractalkine receptor CX(3)CR1 function by targeted deletion and green fluorescent protein reporter gene insertion. *Mol Cell Biol* **20:** 4106–4114

Karsenty G (2000) Role of Cbfa1 in osteoblast differentiation and function. *Semin Cell Dev Biol* **11:** 343–346

Keane-Myers AM, Gause WC, Finkelman FD, Xhou XD, Wills-Karp M (1998) Development of murine allergic asthma is dependent upon B7-2 costimulation. *J Immunol* **160:** 1036–1043

Lambrecht BN, De Veerman M, Coyle AJ, Gutierrez-Ramos JC, Thielemans K, Pauwels RA (2000) Myeloid dendritic cells induce Th2 responses to inhaled antigen, leading to eosinophilic airway inflammation. *J Clin Invest* **106:** 551–559

Le X, Groner Y, Kornblau S, Gu Y, Hittelman W, Levanon D, Mehta K, Arlinghaus R, Chang K (1999) Regulation of AML2/CBFA3 in hematopoietic cells through the retinoic acid receptor alpha-dependent signaling pathway. *J Biol Chem* **274:** 21651–21658

Levanon D, Bernstein Y, Negreanu V, Ghozi MC, Bar-Am I, Aloya R, Goldenberg D, Lotem J, Groner Y (1996) A large variety of alternatively spliced and differentially expressed mRNAs are encoded by the human acute myeloid leukemia gene AML1. *DNA Cell Biol* **15:** 175–185

Levanon D, Bettoun D, Harris-Cerruti C, Woolf E, Negreanu V, Eilam R, Bernstein Y, Goldenberg D, Xiao C, Fliegauf M, Kremer E, Otto F, Brenner O, Lev-Tov A, Groner Y (2002) The Runx3 transcription factor regulates development and survival of TrkC dorsal root ganglia neurons. *EMBO J* **21:** 3454–3463

Levanon D, Brenner O, Negreanu V, Bettoun D, Woolf E, Eilam R, Lotem J, Gat U, Otto F, Speck N, Groner Y (2001a) Spatial and temporal expression pattern of Runx3 (Aml2) and Runx1 (Aml1) indicates non-redundant functions during mouse embryogenesis. *Mech Dev* **109:** 413–417

Levanon D, Glusman G, Bangsow T, Ben-Asher E, Male DA, Avidan N, Bangsow C, Hattori M, Taylor TD, Taudien S, Blechschmidt K, Shimizu N, Rosenthal A, Sakaki Y, Lancet D, Groner Y (2001b) Architecture and anatomy of the genomic locus encoding the human leukemia-associated transcription factor RUNX1/AML1. *Gene* **262:** 23–33

Levanon D, Glusman G, Bettoun D, Ben-Asher E, Negreanu V, Bernstein Y, Harris-Cerrruti C, Brenner O, Eilam R, Lotem J, Fainaru O, Goldenberg D, Pozner A, Wolf E, Xia C, Yarmus M, Groner Y (2003) Phylogenesis and regulated expression of the RUNT domain transcription factors RUNX1 and RUNX3. *Blood Cells Mol Dis* **30:** 161–163

Levanon D, Goldstein RE, Bernstein Y, Tang H, Goldenberg D, Stifani S, Paroush Z, Groner Y (1998) Transcriptional repression by AML1 and LEF-1 is mediated by the TLE/Groucho corepressors. *Proc Natl Acad Sci USA* **95:** 11590–11595

Levanon D, Negreanu V, Bernstein Y, Bar-Am I, Avivi L, Groner Y (1994) AML1, AML2, and AML3, the human members of the *runt domain* gene-family: cDNA structure, expression, and chromosomal localization. *genomics* **23:** 425–432

Li QL, Ito K, Sakakura C, Fukamachi H, Inoue K, Chi XZ, Lee KY, Nomura S, Lee CW, Han SB, Kim HM, Kim WJ, Yamamoto H, Yamashita N, Yano T, Ikeda T, Itohara S, Inazawa J, Abe T, Hagiwara A, Yamagishi H, Ooe A, Kaneda A, Sugimura T, Ushijima T, Bae SC, Ito Y (2002) Causal relationship between the loss of RUNX3 expression and gastric cancer. *Cell* **109:** 113–124

Lutz MB, Suri RM, Niimi M, Ogilvie AL, Kukutsch NA, Rossner S, Schuler G, Austyn JM (2000) Immature dendritic cells generated with low doses of GM-CSF in the absence of IL-4 are maturation resistant and prolong allograft survival *in vivo*. *Eur J Immunol* **30:** 1813–1822

Massague J, Blain SW, Lo RS (2000) TGFbeta signaling in growth control, cancer, and heritable disorders. *Cell* **103:** 295–309

Nathan C (2002) Points of control in inflammation. *Nature* **420:** 846–852

Persson U, Izumi H, Souchelnytskyi S, Itoh S, Grimsby S, Engstrom U, Heldin CH, Funa K, ten Dijke P (1998) The L45 loop in type I receptors for TGF-beta family members is a critical determinant in specifying Smad isoform activation. *FEBS Lett* **434:** 83–87

Pozner A, Goldenberg D, Negreanu V, Le S-Y, Elroy-Stein O, Levanon D, Groner Y (2000) Transcription-coupled translation control of AML1/RUNX1 is mediated by cap- and internal ribosome entry site-dependent mechanisms. *Mol Cell Biol* **20:** 2297–2307

Puig-Kroger A, Sanchez-Elsner T, Ruiz N, Andreu EJ, Prosper F, Jensen UB, Gil J, Erickson P, Drabkin H, Groner Y, Corbi AL (2003) RUNX/AML and C/EBP factors regulate CD11a integrin expression in myeloid cells through overlapping regulatory elements. *Blood*

Schneeberger EE, Vu Q, LeBlanc BW, Doerschuk CM (2000) The accumulation of dendritic cells in the lung is impaired in CD18−/− but not in ICAM-1−/− mutant mice. *J Immunol* **164:** 2472–2478

Shi MJ, Stavnezer J (1998) CBF alpha3 (AML2) is induced by TGF-beta1 to bind and activate the mouse germline Ig alpha promoter. *J Immunol* **161:** 6751–6760

Shortman K, Liu YJ (2002) Mouse and human dendritic cell subtypes. *Nat Rev Immunol* **2:** 151–161

Speck NA (2001) Core binding factor and its role in normal hematopoietic development. *Curr Opin Hematol* **8:** 192–196

Steinman RM (1999) *Dendritic cells, in Fundamental Immunology.* Philadelphia: Lippincott-Raven

Steinman RM, Pack M, Inaba K (1997) Dendritic cells in the T-cell areas of lymphoid organs. *Immunol Rev* **156:** 25–37

Stewart M, MacKay N, Cameron ER, Neil JC (2002) The common retroviral insertion locus Dsi1 maps 30 kilobases upstream of the P1 promoter of the murine Runx3/Cbfa3/Aml2 gene. *J Virol* **76:** 4364–4369

Taniuchi I, Osato M, Egawa T, Sunshine MJ, Bae SC, Komori T, Ito Y, Littman DR (2002) Differential requirements for Runx proteins in CD4 repression and epigenetic silencing during T lymphocyte development. *Cell* **111:** 621–633

Topilski I, Harmelin A, Flavell RA, Levo Y, Shachar I (2002) Preferential Th1 immune response in invariant chain-deficient mice. *J Immunol* **168:** 1610–1617

Umetsu DT, McIntire JJ, Akbari O, Macaubas C, DeKruyff RH (2002) Asthma: an epidemic of dysregulated immunity. *Nat Immunol* **3:** 715–720

Vermaelen KY, Carro-Muino I, Lambrecht BN, Pauwels RA (2001) Specific migratory dendritic cells rapidly transport antigen from the airways to the thoracic lymph nodes. *J Exp Med* **193:** 51–60

Whitehead GS, Walker JK, Berman KG, Foster WM, Schwartz DA (2003) Allergen-induced airway disease is mouse strain dependent. *Am J Physiol Lung Cell Mol Physiol* **285:** L32–42

Woolf E, Xiao C, Fainaru O, Lotem J, Negreanu V, Bernstein Y, Goldenberg D, Brenner O, Levanon D, Groner Y (2003) Runx3 and Runx1 are required for CD8 cell development during thymopoiesis. *Proc Natal Acad Sci USA* **100:** 7731–7736

Yamaguchi Y, Tsumura H, Miwa M, Inaba K (1997) Contrasting effects of TGF-beta 1 and TNF-alpha on the development of dendritic cells from progenitors in mouse bone marrow. *Stem Cells* **15:** 144–153